LM-01K067
August 1, 2001

GaAs Films Prepared by RF-Magnetron Sputtering

L.H. Ouyang, D.L. Rode, T. Zulkifli,
Barbara Abraham-Shrauner, N. Lewis, M.R. Freeman

NOTICE

GaAs Films Prepared by RF-Magnetron Sputtering

L.H. Ouyang, D.L. Rode,[a] T. Zulkifli, and Barbara Abraham-Shrauner
Department of Electrical Engineering, Washington University, St. Louis, Missouri 63130

N. Lewis and M.R. Freeman
Lockheed Martin Corporation, Schenectady, New York 12301

Abstract

We report on the optical absorption, adhesion, and microstructure of RF-magnetron sputtered films of hydrogenated amorphous and microcrystalline GaAs films for the 1 to 25μm infrared wavelength range. Sputtering parameters which were varied include sputtering power, temperature and pressure, and hydrogen sputtering-gas concentration. TEM results show a sharp transition from purely amorphous GaAs to a mixture of microcrystalline GaAs in an amorphous matrix at 34±2°C. By optimizing the sputtering parameters, the optical absorption coefficient can be decreased below $100cm^{-1}$ for wavelengths greater than about 1.25μm. These results represent the lowest reported values of optical absorption for sputtered films of GaAs directly measured by spectrophotometry for the near-infrared wavelength region.

[a] Electronic mail: dlr@ee.wustl.edu

I. Introduction

Numerous applications for compound semiconductors in the areas of microelectronics and optoelectronics have been found.[1] Due to its large electron mobility[2] and high internal quantum efficiency[3] (caused by a direct energy band gap), crystalline GaAs is widely used in microwave transistors and in light-emitting diodes and lasers. On the other hand, thin films of amorphous and microcrystalline GaAs are potentially useful for optical switches and for infrared interference filters.[4]

Interference filters are constructed using alternating layers of large and small refractive-index films, i.e. so-called High/Low filters such as are used in vertical-cavity surface-emitting lasers (VCSELs).[5] A good candidate for the high-index film is GaAs due to its potentially high transparency over the 1 to 20μm wavelength range which is important for fiber optics and quantum-cascade lasers.[6, 7, 8] In comparison to crystalline GaAs, amorphous GaAs can have an even larger index of refraction, and its highly resistive nature avoids the problem of free-carrier absorption.[9] Accordingly, in this work we examine the properties of RF-magnetron sputtered films of hydrogenated amorphous and microcrystalline GaAs, where RF (Radio Frequency) refers to 13.56MHz.

There are several previous studies of GaAs thin-film deposition by RF-diode sputtering,[10, 11, 12] by RF-magnetron sputtering,[13] by glow-discharge sputtering,[14] and by flash evaporation.[15] Sputtering generally yields better optical-quality films in terms of low optical absorption. In particular, RF-diode sputtering of hydrogenated GaAs thin films (GaAs:H) has shown the best promise of producing films with low optical absorption.[16, 17] Due to the many possible sputtering parameters which can be varied, it is difficult to make precise comparisons between different sputtering systems. However, important parameters aside from geometrical factors include sputtering power, temperature and pressure, and hydrogen sputtering-gas concentration as presented below. In addition, the magnetron configuration, as opposed to the diode configuration, is known to minimize electron bombardment damage of the film,[18, 19] and it may be expected to yield significant differences in the optical performance of sputtered films.

Regarding the amorphous *versus* microcrystalline structure of the sputtered films, there are several references in the literature which indicate that the sputtering temperature should be kept sufficiently low to achieve films with predominantly amorphous structure, but reports by different investigators disagree in detail. Murri et al. mention that the substrate temperature should be kept below 4°C to form the amorphous structure and above 25°C to form partly microcrystalline films.[20] Reuter et al. found that GaAs films are predominantly amorphous for substrate temperatures below 200°C and microcrystalline if the substrate temperature is above 300°C.[12] Wang et al. report that sputtering of thin films at 20°C results in an amorphous structure and that polycrystalline GaAs films form at a substrate temperature of 200°C.[21] Hargreaves et al. say that temperatures between 20 and 30°C yield amorphous films and above 200°C yield polycrystalline films.[22] Transmission electron

microscopy (TEM) results obtained by Baker et al. show that the pure amorphous structure forms at a substrate temperature up to about 50°C and a mixture of microcrystalline and amorphous material forms between 72 and 122°C.[23] Paul et al. show by x-ray diffraction analysis that microcrystalline films form above 40°C.[10] Bandet et al. pointed out that the higher the temperature, the smaller the Urbach tail of the optical absorption coefficient.[16] Carchano et al. find amorphous films at substrate temperatures below 50°C using a 10/40mTorr H_2/Ar sputtering gas mixture.[24]

TEM results reported by Bunton and Day show that RF-sputtered amorphous GaAs is formed at 20°C, polycrystalline material forms at 140°C and single-crystal GaAs forms on NaCl substrates above 240°C.[25] The divergence of the sputtering-temperature conclusions may result from differing sputtering apparatus, but the common result is to sputter below about 50°C to form an amorphous structure. In this work, we find a rather sharp transition from purely amorphous GaAs to a mixture of microcrystalline GaAs in an amorphous matrix at 34±2°C for RF-magnetron sputtering in pure Ar gas at 1.5mTorr. Since most of the present work is carried out above this temperature (up to 207°C), it is anticipated that the present films are a mixture of microcrystalline material in an amorphous matrix of GaAs.

It has long been known that hydrogenation greatly reduces the optical absorption of sputtered amorphous silicon.[26] Hydrogen is also important in GaAs films and the optical properties can similarly be affected dramatically.[21, 22, 27] Wang et al. and Carbone et al. find that adding H_2 to the sputtering gas shifts the optical absorption edge to higher photon energies.[21, 28] It has been suggested that atomic hydrogen saturates dangling bonds and decreases the electrical conductivity by several orders of magnitude.[21] Coscia et al. report that hydrogen can induce a rearrangement of the bond angles between Ga and As atoms, reducing bond-angle distortion and the depth of the valence-band tail.[29] The optical absorption edge shifts to higher photon energies with increasing hydrogen concentration, but prolonged annealing above 150°C removes hydrogen from the film.[27] Bandet et al. and Murri et al. suggest that hydrogen saturates dangling bonds.[16, 20] Thus, the optical absorption coefficient will be reduced with added hydrogen during sputtering. The RF sputtering power level is also a critical parameter. Paul et al. indicate that GaAs films are smooth and homogeneous at low RF sputtering power and a few inclusions appear when deposition occurs at higher power (200W).[10] Electron-diffraction patterns show that the structure of GaAs films deposited at higher RF power comprises a poor amorphous quality with elongated agglomerates.[11] Higher RF power levels also yield microcrystalline structure in the case of silicon films.[30] We report below our results on the optical properties of GaAs films sputtered at RF power levels from 400 to 800W.

In the present work, we carried out a series of experiments on RF-magnetron sputtering of GaAs on insulating and conducting substrates with varying sputtering parameters, such as sputtering temperature, pressure and RF power, and various hydrogen concentrations in

the sputtering gas. Regarding the sputtering temperature, we find that optical absorption is reduced for higher sputtering temperatures, or with higher hydrogen partial pressure, or with higher sputtering pressure with constant Ar/H_2 ratio. By optimizing these parameters, the optical absorption coefficient α can be decreased below $100cm^{-1}$ for wavelengths greater than about 1.25μm. These results represent the lowest reported values of optical absorption directly measured by spectrophotometry for the near-infrared wavelength region which is relevant to fiber optics applications.

II. Experimental Procedures

Sputtering System

The sputtering system consists of a Varian 3125H vacuum chamber, with a 50x75mm view-port, containing three RF-magnetron S-guns[18] each with a 130mm diameter conical target spaced 11cm from the substrate holder. The 13.56MHz RF power is delivered to the S-guns by either of two 1,250W RF power supplies (Advanced Energy, Model RFX-1250) through adjustable matching networks. The magnetic field at the dominant sputtering region on the target is 200 ± 20G as measured by a gauss-meter (Bell, Model 640). The single-crystal undoped semi-insulating GaAs target with 30° off-(100) orientation (supplied by Litton/Airtron) is installed in the water-cooled S-gun using a Ga-In eutectic alloy backing for good thermal contact. Thermal shock (i.e. target fracture) was found to be a major difficulty in this work, but the eutectic alloy helped a great deal. The GaAs target material is estimated to be pure to better than 1ppm. The vacuum environment is monitored by a residual gas analyzer (Veeco, Model SPI-10 monopole mass spectrometer).

The 600-liter vacuum system is pumped by a direct-drive 1500l/m chemical pump (Leybold-Heraeus Trivac, Model D65BCS) backing a 450l/s turbomolecular pump (Balzers, Model TPU450H). A liquid-nitrogen trap provides improved background water-vapor pumping. The vacuum system has an ultimate unbaked background pressure of $2x10^{-7}$ Torr consisting predominantly of water vapor. High-purity Ar and Ar/H_2 mixtures (5-9s pure) are provided through 200sccm mass-flow controllers (MKS, Model 2259C) and stainless-steel lines. Sputtering pressure is set by holding the gas flow constant while partly closing a shutter valve over the pumping stack.

Four quartz-halogen lamps (GE, Model Q6.6AT4/5CL) provide up to 800W of radiant-heating power from a proportional controller (Varian, Model 980-1203) which is used for regulating the substrate-holder temperature. The copper substrate holder can be heated up to 400°C. We have used stainless steel, graphite, and copper substrate holders but prefer copper for better thermal conductivity and temperature uniformity. The substrate holder contains six 25mm-diameter holes with 500μm wide by 500μm thick retention lips for holding the substrates only near their edges. A solid copper cylinder sits on top of each

substrate in a sputter-up configuration. The substrate-holder temperature is monitored using type-J thermocouples.

Various Ar/H_2 mixtures from pure Ar to 75% H_2 are selected to explore the effects of hydrogen. Total sputtering pressure ranges from 2 to 20mTorr as monitored by an absolute-pressure manometer (Baratron, Model 628B). The RF power ranges up to 800W. Due to the high sensitivity to thermal shock for the GaAs target, most experiments are done at 400W. Film thicknesses vary between 0.6 and 6.8μm. The samples have a thickness uniformity of about 8% over the 150mm diameter substrate holder.

Substrates

We have used the following types of substrates: glass microscope slips (borosilicate, Corning #0211), single-crystal sapphire, silica (low-hydroxyl, Suprasil 300), single-crystal (100) InP, ZnSe, Si, and GaAs. The slips, silica, and sapphire substrates allow for measurements in the near-infrared and visible wavelength regions while InP, ZnSe, Si, and GaAs allow for near and medium-infrared measurements. Substrates are 25mm in diameter with thicknesses of 220μm (slips), 330μm (sapphire), 2370μm (silica), 480μm (InP), 540μm (ZnSe), 520μm (Si), and 600μm (GaAs).

Substrate cleaning was carried out by dipping and swabbing in a 5:1 sulfuric-acid:deionized water (18MΩ) mixture followed by a deionized water rinse and filtered high-purity N_2 blow-dry. The substrates are then baked at 120°C for 1 hour and are usually loaded into the vacuum system within 3 hours, although we have not noticed any different results after as much as a 24-hour delay. Substrates are occasionally inspected for cleanliness using dark-field microscopy (Zeiss, Model 465-2833). After the substrates are loaded into the vacuum system and pumped down below $6x10^{-7}$Torr, they are *in-situ* baked at 200°C for at least 1 hour prior to sputter deposition or back-sputtering.

Transmission Electron Microscopy

Conclusions reported by Murri et al. show that sputtered GaAs films contain both amorphous and microcrystalline structures depending on the sputtering parameters.[20] In order to examine the microstructure of sputtered films with different sputtering parameters, ion-milled cross-sections of GaAs samples were observed by transmission electron microscopy (TEM) in a Philips EM420 analytical electron microscope. The samples measured 100±50nm thick.

Film Thickness Measurement

Since we wish to determine the index of refraction to an accuracy of 2% and the optical absorption coefficient α down to $100cm^{-1}$ in films which are 2μm thick, it is necessary to know the film thickness to an accuracy of 2% and to measure the optical transmittance to an accuracy of better than 2%. Therefore, we need to determine the thickness of 2μm films accurately to within 40nm. We have had poor success using the mechanical-stylus techniques which are mentioned in the literature, i.e. etched, masked or fractured step-height measurements using surface profilometry (Sloan Dektak instrument) due to poor film adhesion at step edges, or due to etching into the substrate, or due to film thickness taper at masked steps. We find these methods to be accurate to 40nm in rare circumstances and 150nm is not unusual for 2μm and greater thicknesses.

Consequently, because of its importance to accuracy, we introduce here a new technique which we have found to be accurate to 30nm on a regular basis, i.e. hundreds of samples. The method resembles that introduced by Holonyak.[31] A cylindrical sectioning machine (Philtec, Model 2015C) provides a shallow lapped groove through the film and slightly into the substrate using 1μm diamond paste. See Fig. 1. The interference fringe-shift of the lapped sample is measured with Michelson interferometry using Na^D-line illumination (589.3nm wavelength). The Michelson interferometer consists of a microscope (Reichert, Model 323701) with a Michelson interferometer attachment (Watson Barnet, 16mm). Fig. 1a shows a photomicrograph of the interferogram. The fringe shift shown by the fine white line indicates a fringe shift of N = 6.7 fringes so that the film thickness d can be obtained from the equation d = 589.3xN/2, or 1.97μm in this case. The fringe shift can be ascertained to within 1/10 of a fringe, corresponding to a precision of ±30nm. The Na^D-line filter has been measured to an accuracy of 0.4nm, or 0.07%.

Film Adhesion and Delamination

As-deposited GaAs films are under strong compression, i.e. about $3x10^9 d/cm^2$, and this leads to problems with film adhesion and delamination from the substrate when films exceed about 0.8μm in thickness. We find that 1h, 200°C baking and substrate back-sputtering at -70V prior to film deposition and, in some cases, bias-sputtering greatly improves adhesion on most substrates. Bias-sputtering improves the structure and adhesion of aluminum films on Si.[32]

III. Experimental Results

Sample Preparation

In this work, we studied the optical absorption coefficient α, film adhesion and microstructure of RF-magnetron sputtered hydrogenated GaAs films (GaAs:H) while varying four different sputtering parameters. The parameters are: substrate-holder

temperature T_s during sputtering, total sputtering-gas pressure P_{tot}, H_2 partial pressure in the H_2/Ar sputtering gas mixture P_H, and the RF sputtering power P_{RF}.

We selected 18 samples from over 200 to examine different sputtering effects. Table I shows the sample data. For example, the average sputtering temperature T_s is 200±5°C for some of the RF-power and pressure experiments. We set the substrate-holder temperature to 195°C before sputtering, and the temperature increased by 10°C during sputtering. Hence the variation is ±5°C.

Table I. Sample data for various sputtering parameters.

Sample No.	T_s (°C)	P_{RF} (Watts)	P_{tot} (mTorr)	P_H (mTorr)	Thickness (μm)
01219E	200±5	400	10.0	2.5	2.19
01220E	169±5	400	10.0	2.5	2.03
01221F	149±5	400	10.0	2.5	2.31
01222F	106±10	400	10.0	2.5	2.16
10323C	198±5	400	2.25	0.56	1.24
10326D	196±1	400	5.00	1.25	1.50
10330D	195±4	400	10.0	2.5	2.27
10328D	200±5	400	20.0	5.0	2.21
10213B	157±5	400	10.0	5.0	2.36
10124C	151±4	400	10.0	7.5	2.36
01012C	191±3	400	10.0	2.5	2.27
01108C	207±15	650	10.0	2.5	2.27
01031B	205±14	800	10.0	2.5	2.42
10405E	35±10	400	20.0	5.0	1.16
00820A	35±10	400	2.25	0.56	2.06
00803C	35±10	400	2.25	0.56	1.49
10206B	156±5	400	2.25	1.69	1.15
9020801	35±12	800	1.50	0	0.78

Sputtering Rate

The average sputtering rate (total thickness divided by total sputtering time) is affected by changing the deposition parameters. Michelson interferometry measurements show that the sputtering rate decreases as the hydrogen partial pressure increases. See Fig. 2. The three GaAs films were all sputtered at 10mTorr total sputtering pressure, but with different H_2/Ar ratios. The results show that reduced hydrogen yields higher sputtering rates under constant total sputtering pressure. These results are consistent with those of Murri et al. for GaAs films fabricated by RF-diode sputtering.[17, 29] Alimoussa et al. conclude that hydrogen, in addition to having a lower sputtering yield due to its small mass, reduces the

concentration of ionized Ar, even though the ionization potentials for atomic hydrogen and for H_2 are 13.6 eV and 15.42eV respectively, which is quite similar to Ar, i.e. 15.76 eV.[33] A similar result by Freeman et al. indicates that the sputtering rate of silicon films is decreased by increasing the hydrogen concentration.[34] The explanation that hydrogen atoms provide less-efficient momentum exchange with target atoms due to their relatively small atomic mass, and thus reduced sputtering yield, seems reasonable. Higher Ar sputtering pressure alone results in lower sputtering rates as shown by Fraser[19] for DC-magnetron sputter-deposition of aluminum thin films, a result which we have confirmed for RF-magnetron sputtering of Al in pure Ar. Vapor-phase atom and ion scattering are increased due to reduction of the mean-free-path under increased sputtering pressure conditions, leading to reduced transport of material from the target to the substrate and, hence, a diminished sputtering rate.

Aside from the foregoing, there may be a novel explanation as follows. We have noticed a significant decrease (a few percent) in the total pressure when the plasma is ignited and sputtering commences provided that the H_2 concentration is 75%, but not if pure Ar is used. This is almost certainly due to the pumping of H_2 into the freshly sputtered layer at the surfaces of the vacuum chamber analogous to the mechanism known as[35] "sublimation pumping." Due to the small mass and high reactivity of certain hydrogen species and this pumping effect, hydrogen will diffuse more rapidly than Ar and the plasma density might thus be substantially reduced in H_2/Ar mixtures in comparison to pure Ar.

Surface Morphology & Film Adhesion

The surface morphology of GaAs sputter-deposited in pure Ar and in 25% H_2 is optically smooth. Fig. 3 is a photomicrograph of the surface of Sample #01219E in Nomarski contrast which is capable of revealing 10nm surface features. The surface can be seen to be featureless. Fig. 4 is an AFM (Atomic Force Microscope) photomicrograph of Sample #10405E. The scanning area is 1x1μm, and the rms roughness of the film is about 4.2nm, which is quite satisfactory for optical applications.

Delamination at the film-substrate interface degrades optical transmittance due to multiple reflections, and poor adhesion complicates the fabrication of multi-layer structures. Some common examples of adhesion problems are shown in the Nomarski-contrast photomicrographs of Figs. 5 and 6. Figs. 5a and b were both taken from the same sample, but Fig. 5b was taken seven months after Fig. 5a. The small circular features in Fig. 5a are approximately 25μm in diameter and appear to be lenticular blisters which have delaminated from the substrate, and most of them have broken away around the periphery of the blister. Tiny shards of film are sometimes found in the film storage containers due to this effect. We rarely see this mode of failure if the films are thinner than 0.8μm. Hence, we feel it is probably due to a strong compressive stress in the film.

Interestingly, after seven months in air at room temperature (in a Teflon® storage canister, Entegris/Fluoroware, Model H22-20-0615) as shown in Fig. 5b, larger features appear. These 60μm circular features are again regions of delamination where the film has entirely broken away from the substrate. It is unknown whether this might be caused by nucleation and growth from trapped gas in the film, or if it is simply delamination leading to stress relief. Also, we are not sure whether the large blisters are new features, or whether they are evolutions of the small features seen in Fig. 5a. (The latter seems unlikely in view of the stability of the small features seen in Fig. 5 over a period of seven months.) In either case, they appear to be caused by compressive stress in the as-deposited film.

A final example of inadequate film adhesion is shown in Fig. 6 where we have attempted to cylinder-lap a 1.49μm GaAs film in preparation for a thickness measurement. The film has delaminated from the substrate in the lapped area as well as far-removed from the lapped area. Substrate baking before film deposition, back-sputtering and bias sputtering lead to greatly improved adhesion and largely eliminated these problems for film thicknesses up to about 3μm.

We have also observed a unique film failure mechanism for higher H_2 and for high total pressure sputtering which we call a "shaling" effect, i.e. it resembles a fine-grained rock which splits into thin layers when fractured. Fig. 7 is a Michelson interferogram of a sample where the lighter part is the surface of the GaAs film and the darker part is the residual GaAs film after the upper layer has partly peeled off to a depth of about 1μm. The fringes on both sides of the fracture are parallel, indicating that there is a sharp step-height difference. The shaled area is considerably rougher, as shown by the low-contrast interference fringes. This occurs commonly in thicker samples with 75/25% H_2/Ar sputtering gas mixtures for total sputtering pressures above 15mTorr. The films split into thin sheets during sputtering and shale off. The structure of the film is probably weakened by the high percentage of hydrogen, and it is still under significant compressive stress. This results in the shaling effect. It is also possible that this peculiar structure occurs due to film delamination from the substrate during sputtering with the delaminated areas subsequently being further covered by additional sputtering, but the surface and edge morphology shown in Fig. 6 suggest that this is not the case. In general, samples sputtered in 50 and 75% H_2 have more hazy (rougher) surfaces that worsen with increasing sputtering pressure over 10mTorr.

Optical Properties

In order to derive the optical absorption coefficient α from spectrophotometric measurements, the optical transmittance of GaAs films was measured with 2% precision by spectrophotometry (sample-in, sample-out method) as discussed in detail elsewhere.[36] For the first series of samples, we varied the sputtering temperature from 109 to 200°C while

holding the RF-sputtering power and total pressure constant at 400W and 10mTorr (25% H_2/75%Ar) as shown in Fig. 8. The smallest values of α occur for Sample #01219E which was sputtered at 200°C. We anticipate, as in the case of amorphous Si,[26] that deposition at higher temperatures will lead to less hydrogen in the film due to a reduced hydrogen sticking coefficient, and there will be a greater proportion of microcrystalline material in the amorphous matrix. While decreased hydrogen would have been expected to increase α, conversion from amorphous to microcrystalline material seems to decrease it at an even greater rate as the sputtering temperature is increased, leading to an overall reduction in the optical absorption coefficient.[37]

A photomicrograph of a TEM cross-section of a GaAs film is shown in Fig. 9. The GaAs film (Sample #9020801) was deposited onto a single crystal (100) semi-insulating GaAs substrate in 1.5mTorr of pure Ar with 800W of RF power. The photomicrograph shows that a 0.34μm thick amorphous GaAs layer was deposited adjacent to the substrate, and subsequently microcrystalline material in an amorphous matrix grew on top of the purely amorphous layer. Since the sputtering deposition began at a temperature of 24°C and ended at a temperature of 47°C, the temperature at the point of conversion from pure amorphous material to the mixed phase is estimated to be 34±2°C. The sharpness of the interface between the amorphous phase and the mixed amorphous/microcrystalline phase indicates that the transition between the two phases occurred suddenly.

In the next series of experiments, GaAs films were sputtered with varying total sputtering pressure at 200°C in 25%H_2/75%Ar at 400W RF-power. The results in Fig. 10 show that higher pressure leads to lower optical absorption coefficient α. Sample #10328D which was sputtered at 20 mTorr exhibits a projected α below 100 cm^{-1} for wavelengths beyond 1300nm. (The present spectrophotometric technique can resolve α only down to about 100cm^{-1}.) The hydrogen concentration in the GaAs film increases with H_2 sputtering-gas partial pressure. There are suggestions in the literature that α is reduced because hydrogen saturates dangling bonds emanating from Ga and As atoms.[21] We merely wish to point out that some of the present optical absorption coefficients are lower than any reported in the literature by direct measurement, i.e. not inferred from photo-thermal measurements, for example.

The optical absorption coefficient is also affected by the RF-sputtering power. Fig. 11 shows results for samples sputtered at 400, 650, and 800W in 10mTorr of 25% H_2/75%Ar at 205°C. The results show that higher sputtering powers yield lower optical absorption coefficients. The surface morphology of the 800W film as viewed by Nomarski-contrast optical microscopy exhibits the same smoothness and flatness as samples which were deposited at 400W. The present results are compared with literature values[16, 17, 23, 38] in Fig. 12. Results from Murri et al.[17] were derived from photothermal deflection spectroscopy (PDS) measurements. Those by Bandet et al.[16] were determined using spectrophotometry. Those by Flohr and Helbig[38] were determined using photo-acoustic

spectroscopy (PAS). The results by Baker et al.[23] were determined using spectrophotometry. In addition, we have measured optical absorption of several films out to 25μm wavelengths by means of FTIR (Fourier Transform Infra-Red) spectroscopy and find that α is too small to measure, i.e. less than $100cm^{-1}$. As one can see, the optical absorption coefficient for Sample #01031B exhibits the lowest values for α in Fig. 12 by direct measurement, i.e. spectrophotometry.

IV. Discussion

The general behavior of the optical absorption coefficient appears to be determined primarily by two opposing effects: conversion from more highly absorbing amorphous material to less-absorbing microcrystalline material at higher sputtering temperatures, on the one hand, and decreasing hydrogen sticking coefficient and decreasing hydrogen concentration in the film at higher sputtering temperatures on the other hand. Reduced hydrogen concentration causes the absorption coefficient to increase while conversion to the microcrystalline structure causes it to decrease. With more hydrogen in the sputtering environment, the resulting higher hydrogen concentration is thought to cause saturation of more dangling bonds by atomic hydrogen.[20,21] Murri et al. pointed out that hydrogen cannot saturate wrong bonds.[17] It may also be true that distorted bond angles between Ga and As are relaxed in GaAs:H films due to increased mobility of surface-adsorbed species during film deposition along the lines of observation made for Si films.[30] This might also affect the depth of the valence-band tail.[29] Our results are in general agreement with those in the literature.[16, 20, 27, 28, 29, 39]

The experimental series of samples with all sputtering parameters held constant while the sputtering pressure is increased with a 25%H_2/75%Ar mixture may suggest that increasing hydrogen concentration in the films causes decreasing optical absorption. On the other hand, it is noteworthy that the logarithm of the optical absorption coefficient at 1,300nm wavelength falls quite linearly with the total sputtering pressure, indicating that mean-free-path considerations are important, i.e. the flux of energetic neutral hydrogen reflected, after charge exchange, from the target and impinging on the film will decrease exponentially with increasing total pressure. Thus, bombardment of the film by atomic hydrogen during deposition will decrease exponentially with increasing total sputtering pressure. Reduced bombardment at higher pressure may promote microcrystalline structure at the expense of amorphous structure and, hence, reduced optical absorption.

Samples sputtered at higher RF power levels also show significant reductions in optical absorption. Fortunately, in our case, this does not appear to be accompanied by a degradation in surface morphology on the visible wavelength scale.[10] We are not sure of the reasons for this reduction in α. It may result from structural changes during sputtering brought on by increased concentrations of surface-adsorbed hydrogen when the RF-power

is larger. This has been suggested in connection with improved microcrystalline Si:H films which are achieved at higher power levels.[30] One may further note that inefficient transfer of momentum, and thus kinetic energy, from hydrogen atoms to target atoms will lead to a significant increase in energetic hydrogen atom bombardment of the film at higher hydrogen partial pressures because of charge exchange at the target. Hydrogen ions undergo neutralization due to charge exchange at the target and subsequently impinge on the film as energetic neutral hydrogen atoms. The self-bias voltage of the target at 800W RF power is 480±20V, so energetic neutral hydrogen atoms may be implanted up to 5nm into the film surface leading to greater hydrogen incorporation at higher RF power levels, and hence reduced optical absorption.

V. Conclusions

In order to achieve low optical absorption in magnetron sputtered GaAs films, several sputtering parameters must be accurately controlled. The present results show that higher sputtering temperatures, higher sputtering pressures, and higher sputtering power levels, along with hydrogen in the sputtering environment, all act to reduce the optical absorption coefficient. However, the optical absorption coefficient achievable by means of magnetron sputtering appears unlikely to fall to the level needed for optical distribution in planar-waveguide optoelectronic integrated-circuits,[40] i.e. $0.1cm^{-1}$. On the other hand, the present levels of optical absorption are quite interesting in connection with infrared interference filters for the 1 to 10μm wavelength range, and there may also be potential applications for electroöptically-active optical switches.

Clearly, additional work is needed to clarify the relationships between microstructure, sputtering parameters, and optical properties such as index of refraction and absorption coefficient.

References

[1] A.A. Bergh, Compound Semiconductor Magazine **6**, 36 (2000).
[2] D.L. Rode, Semiconductors & Semimetals **10**, 1 (1975).
[3] R.J. Nelson and R.G. Sobers, Appl. Phys. Lett. **32**, 761 (1978).
[4] S. Schön, M. Haiml, and U. Keller, Appl. Phys. Lett. **77**, 782 (2000).
[5] J.J. Wierer, D.A. Kellogg, and N. Holonyak, Appl. Phys. Lett. **77**, 782 (2000).
[6] S. Barbieri, C. Sirtori, H. Page, M. Stellmacher, and J. Nagle, Appl. Phys. Lett. **78**, 282 (2001).
[7] D. Hofstetter, M. Beck, T. Aellen, and J. Faist, Appl. Phys. Lett. **78**, 396 (2001).
[8] J. Faist, F. Capasso, D.L. Sivco, C. Sirtori, A.L. Hutchinson, and A.Y. Cho, Science **264**, 553 (1994).
[9] H.C. Casey, Jr., D.D. Sell, and K.W. Wecht, J. Appl. Phys. **46**, 250 (1975).
[10] D.K. Paul, J. Blake, G. Moddel, and W. Paul, SPIE **346**, 95 (1982).
[11] R. Murri, F. Gozzo, N. Pinto, L. Schiavulli, C. De Blasi, and D. Manno, J. Non-Cryst. Solids **127**, 12 (1991).
[12] H. Reuter, H. Schmitt, and M. Böffgen, Thin Solid Films **254**, 96 (1995).
[13] K. Kumabe and N. Matsumoto, Jpn. J. Appl. Phys. **19** Suppl. 19-2, 119 (1980).
[14] K. Aguir, M. Hadidou, P. Lauque, and B. Despax, J. Non-Cryst. Solids **113**, 231 (1989).
[15] V. Manorama, P.M. Dighe, S.V. Bhoraskar, V.J. Rao, P. Singh, and A.A. Belhekar, J. Appl. Phys. **68**, 581 (1990).
[16] J. Bandet, J. Frandon, G. Bacquet, K. Aguir, B. Despax, and A. Hadidou, Phil. Mag. **B58**, 645 (1988).
[17] R. Murri, L. Schiavulli, N. Pinto, and T. Ligonzo, J. Non-Cryst. Solids **139**, 60 (1992).
[18] P.J. Clarke, U.S. Patent 3,616,450 (1971).
[19] D. B. Fraser, in *Thin Film Processes*, p. 115 (eds. J.L. Vossen and W. Kern, Academic Press, 1978).
[20] R. Murri and N. Pinto, in *Properties of Gallium Arsenide*, p. 155 (eds. M.R. Brozel and G.E. Stillman, IEE Press, 1996).
[21] Z.P. Wang, L. Ley, and M. Cardona, Phys. Rev. **B26**, 3249 (1982).
[22] M. Hargreaves, M.J. Thompson, and D. Turner, J. Non-Cryst. Solids **35&36**, 403 (1980).
[23] S.H. Baker, S.C. Bayliss, S.J. Gurman, N. Elgun, J.S. Bates, and E.A. Davis, J. Phys.: Condens. Matter **5**, 519 (1993).
[24] H. Carchano, K. Sedeek, and J.L. Seguin, in Proc. Euroforum— New Energies Congress **3**, 197 (H.S. Stephens and Assocs., Brussels, 1988).
[25] G.V. Bunton and S.C.M. Day, Thin Solid Films **10**, 11 (1972).
[26] P.J. Zanzucchi, C.R. Wronski, and D.E. Carlson, J. Appl. Phys. **48**, 5227 (1977).
[27] D.K. Paul, J. Blake, S. Oguz, and W. Paul, J. Non-Cryst. Solids **35**, 501 (1980).
[28] A. Carbone, F. Demichelis, G. Kaniadakis, F. Gozzo, R. Murri, N. Pinto, L. Schiavulli, G. Della Mea, A. Drigo, and A. Paccagnella, Il Nuovo Cimento **13D**, 571 (1991).
[29] U. Coscia, R. Murri, N. Pinto, and L. Trojani, J. Non-Cryst. Solids **194**, 103 (1996).
[30] J.E. Gerbi and J.R. Abelson, J. Appl. Phys. **89**, 1463 (2001).
[31] N. Holonyak, Jr., B.A. Vojak, R.M. Kolbas, R.D. Dupuis, and P.D. Dapkus, Solid-State Electron. **22**, 431 (1979).
[32] J.L. Vossen and J.J. O'Neill, Jr., RCA Review **29**, 566 (1968).
[33] L. Alimoussa, H. Carchano, and J.P. Thomas, J. Phys.(Paris) **C4-42**, 683 (1981).
[34] E.C. Freeman and W. Paul, Phys. Rev. **B20**, 716 (1979).
[35] R. Glang, in *Handbook of Thin Film Technology*, p. 1-41 (eds. L.I. Maissel and R. Glang, McGraw-Hill, 1970).
[36] T. Zulkifli, unpublished.
[37] See, for example, Bandet et at., ref. 16.
[38] T. Flohr and R. Helbig, J. Non-Cryst. Solids **88**, 94 (1986).
[39] A.W.R. Leitch and J. Weber, Phys. Rev. **B60**, 13265 (1999).
[40] C.W. Phelps, T.S. Barry, D.L. Rode, and R.R. Krchnavek, IEEE J. Lightwave Techn. **15**, 1900 (1997).

Fig. 1. (a) Photomicrograph of a Michelson interferogram of a cylinder-lapped GaAs sputtered film. The fringe shift is 6.7 as indicated by the white line intersecting the fringes. (b) Schematic cross-section of the sample shown in (a).

Fig. 2. Sputtering rate versus hydrogen partial pressure of the sputtering gas. All films were sputtered at 10mTorr total sputtering-gas pressure but at 0, 25, 50, and 75% H_2 concentration in Ar. The results show that the highest sputtering rate is 7.8Å/s at 0%H_2/100%Ar.

Fig. 3. Nomarski-contrast photomicrograph of a sputtered GaAs film (Sample #01219E) on a slip substrate. The morphology shows that the film is optically smooth on a scale of 10nm.

Fig. 4. Photomicrograph of an AFM image (Sample #10405E) of a GaAs film on a slip substrate. The image area is 1x1μm. The RMS roughness of the sputtered GaAs film surface is about 4.2nm.

Fig. 5. (a) Nomarski-contrast photomicrograph of a sputtered GaAs film (Sample #00820A) showing delamination blisters. (b) Nomarski-contrast photomicrograph of Sample #00820A taken seven months after part (a). Either the delamination is worsening or new blisters are forming with time.

Fig. 6. (a) Nomarski-contrast photomicrograph of a sputtered GaAs film (Sample #00803C) showing poor adhesion after cylinder-lapping. Adhesion can be improved by back-sputtering or bias-sputtering. (b) Schematic cross-section of Sample # 00803C.

Fig. 7. Photomicrograph of a Michelson interferogram of a GaAs film (Sample #10206B) sputtered with a 75%H_2/25%Ar mixture. The lighter part is the smooth upper GaAs film surface and the darker part is the residual GaAs film remaining after the upper part of the layer has peeled off.

Fig. 8. Optical absorption coefficient of sputtered GaAs:H films on slip substrates for sputtering temperatures from 109 to 200°C with 10mTorr of 25%H_2/75%Ar.

Fig. 9. TEM cross-section photomicrograph of a sputtered GaAs film on a single-crystal GaAs substrate. The amorphous structure forms at the beginning of sputtering, followed by a transition to microcrystalline GaAs in an amorphous matrix. The transition occurs at a sputtering temperature of 34±2°C for sputtering in 1.5mTorr of pure Ar.

Fig. 10. Optical absorption coefficient of GaAs:H films sputtered at 200°C on slip substrates for sputtering pressures from 2.25 to 20mTorr. The optical absorption coefficient is reduced for films sputtered at higher sputtering pressures in 25%H_2/75%Ar.

Fig. 11. Optical absorption coefficient of GaAs:H films sputtered at 205°C on slip substrates at a sputtering pressure of 10mTorr versus RF-sputtering power. Higher power yields lower absorption.

Fig. 12. Comparison of the optical absorption coefficient of Sample #01031B with results from the literature. Murri's data were obtained by photothermal deflection spectroscopy, and Flohr's by photoacoustic spectroscopy. The rest were measured by spectrophotometry. The lowest optical absorption coefficient measured directly by spectrophotometry is exhibited by Sample # 01031B.

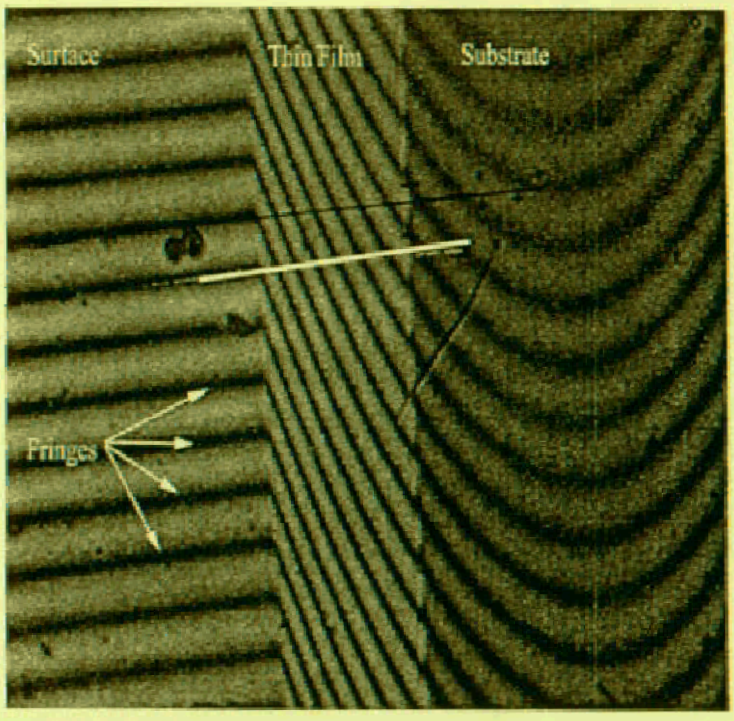

Figure 1a

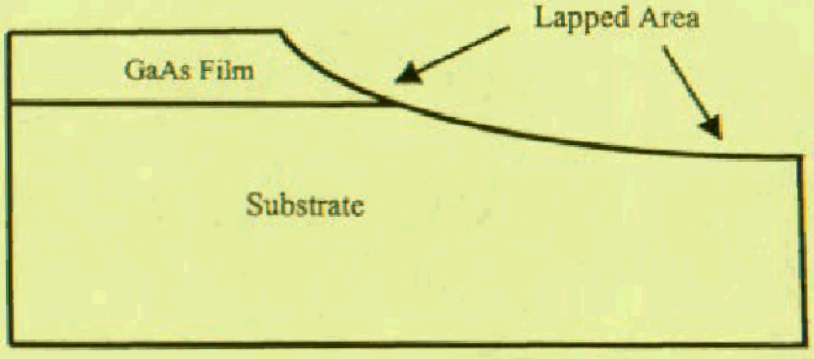

Figure1b

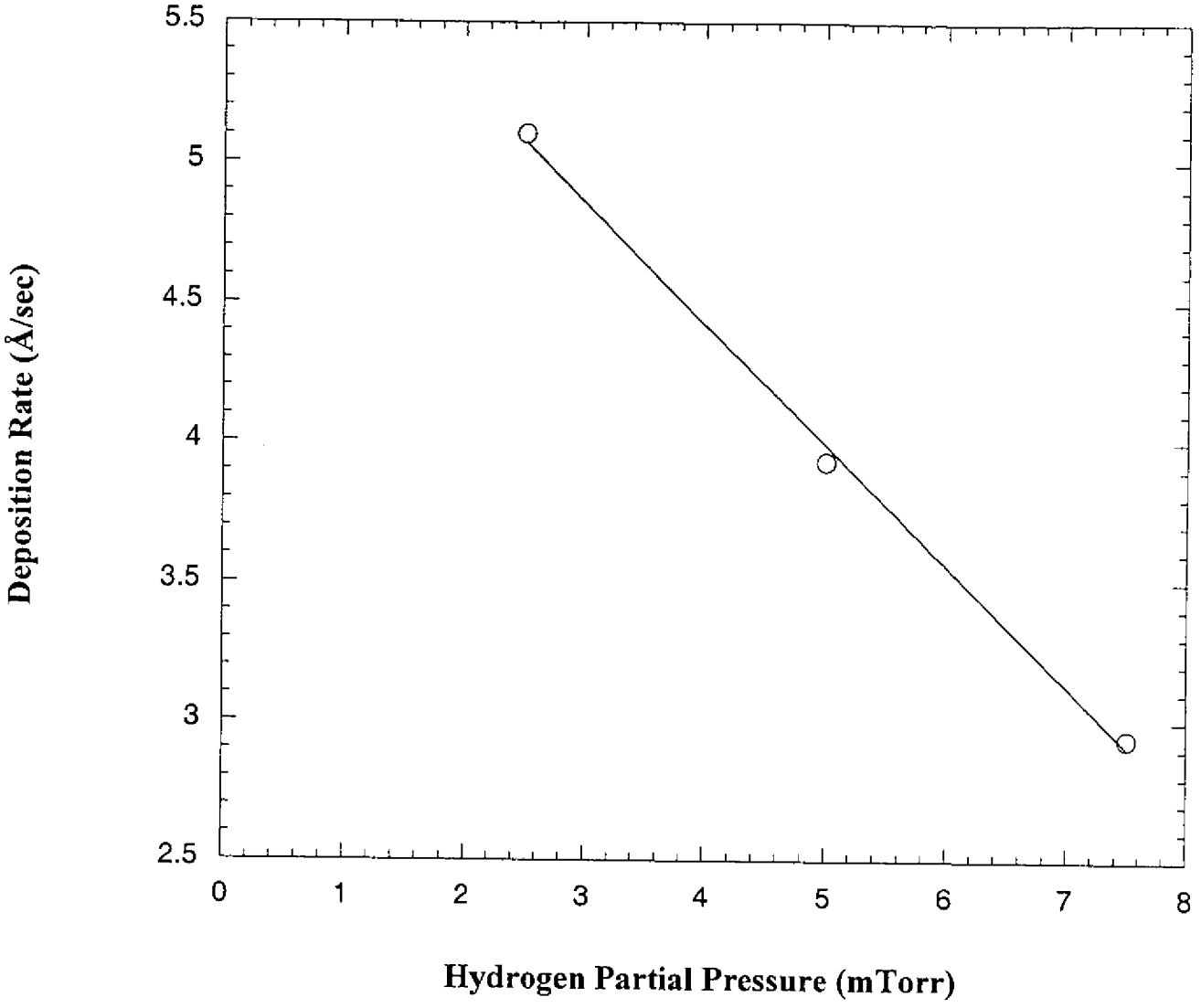
Deposition Rate (Å/sec)
5.5
5
4.5
4
3.5
3
2.5
0
1
2
3
4
5
6
7
8
Hydrogen Partial Pressure (mTorr)

Figure 2

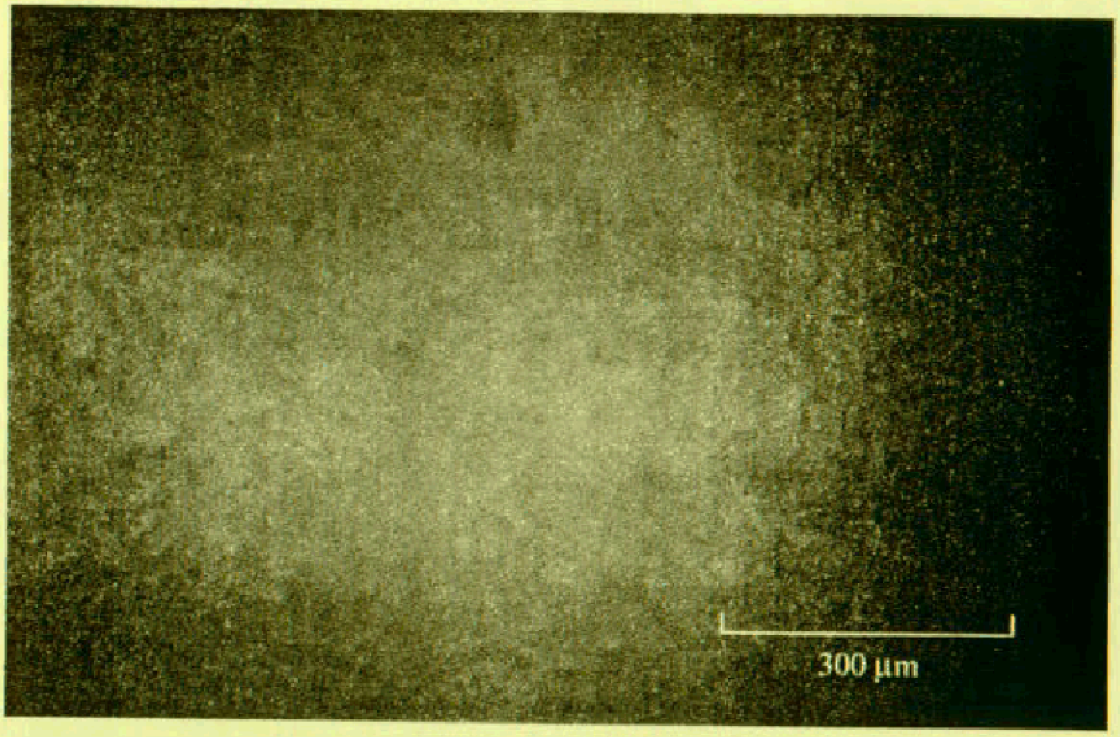

Figure 3

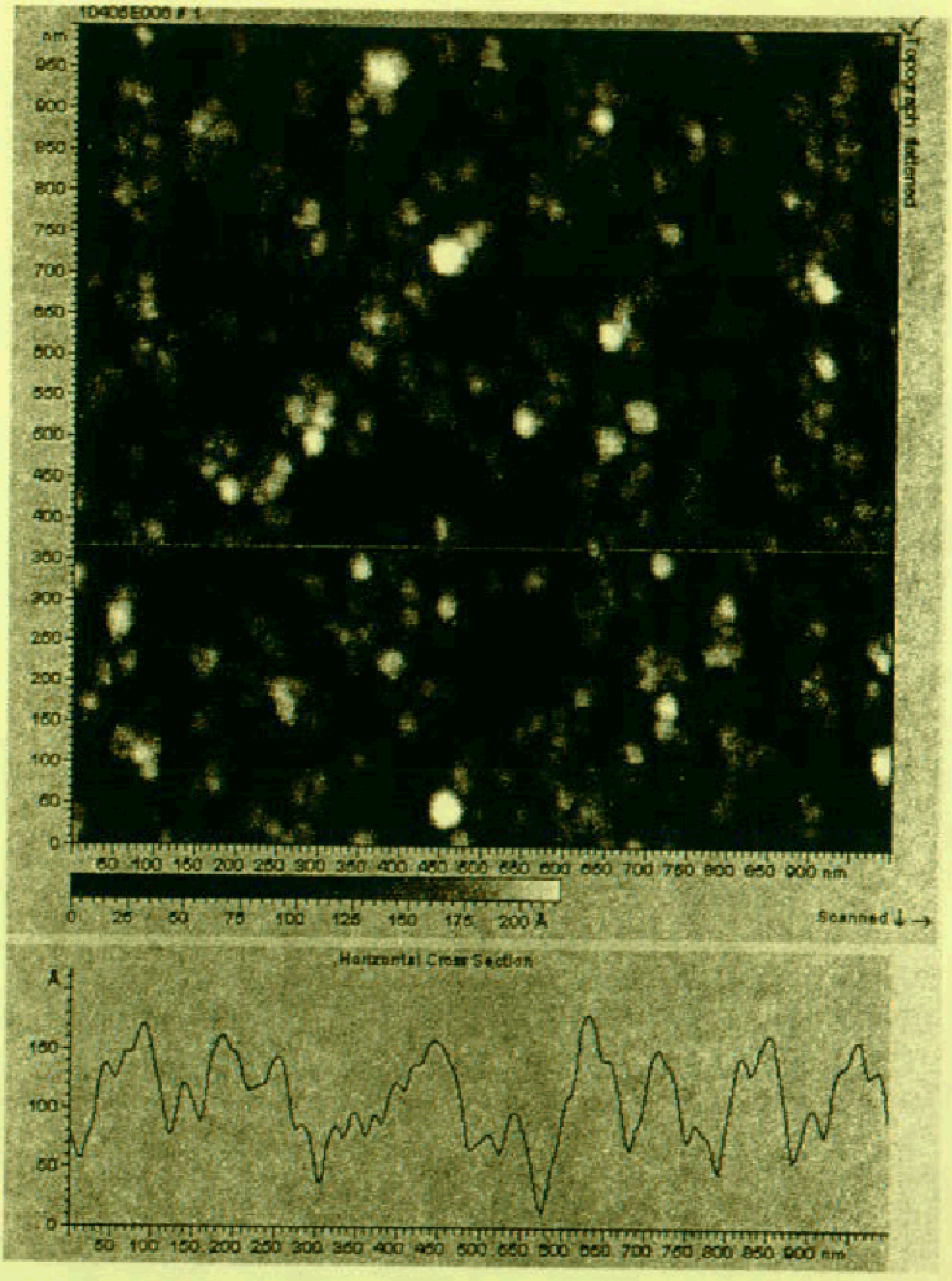

Figure 4

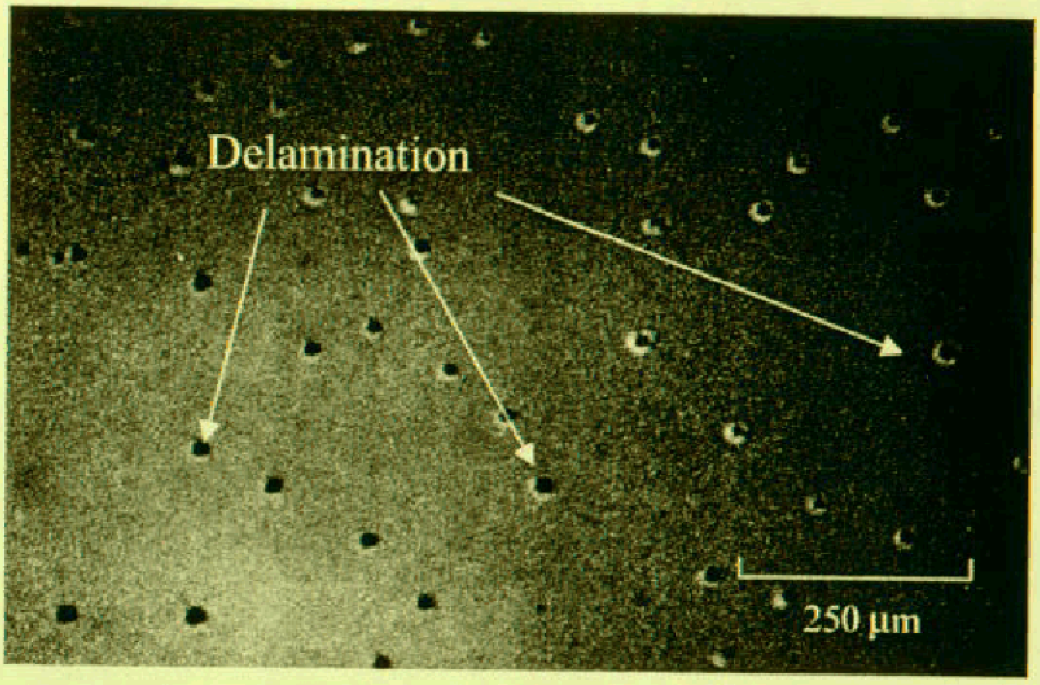

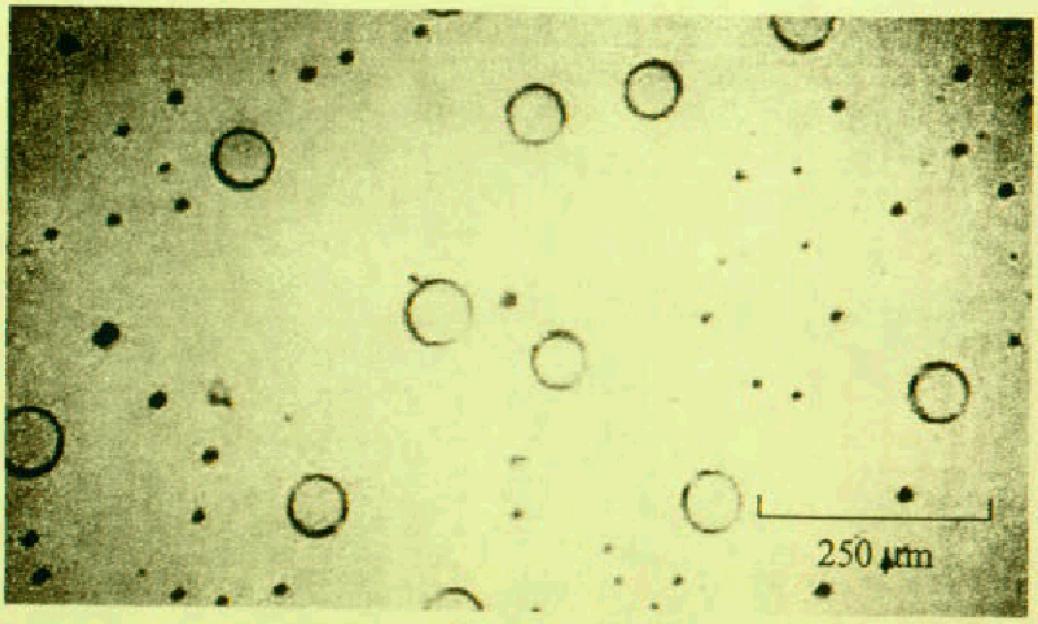

Figure 5

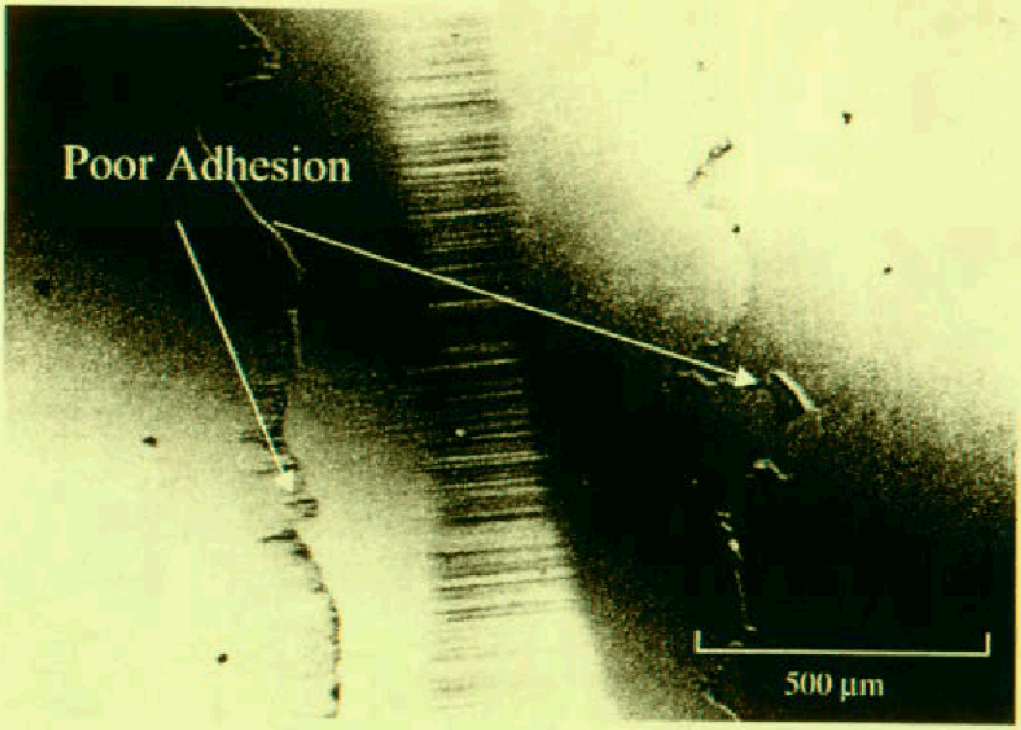

Figure 6a

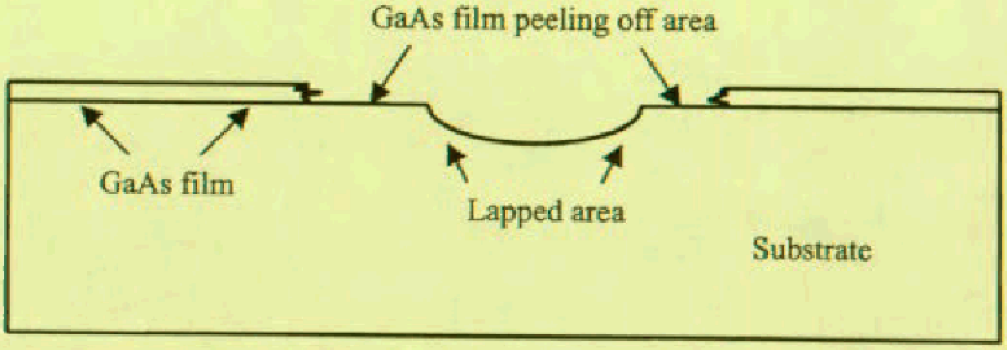

Figure 6b

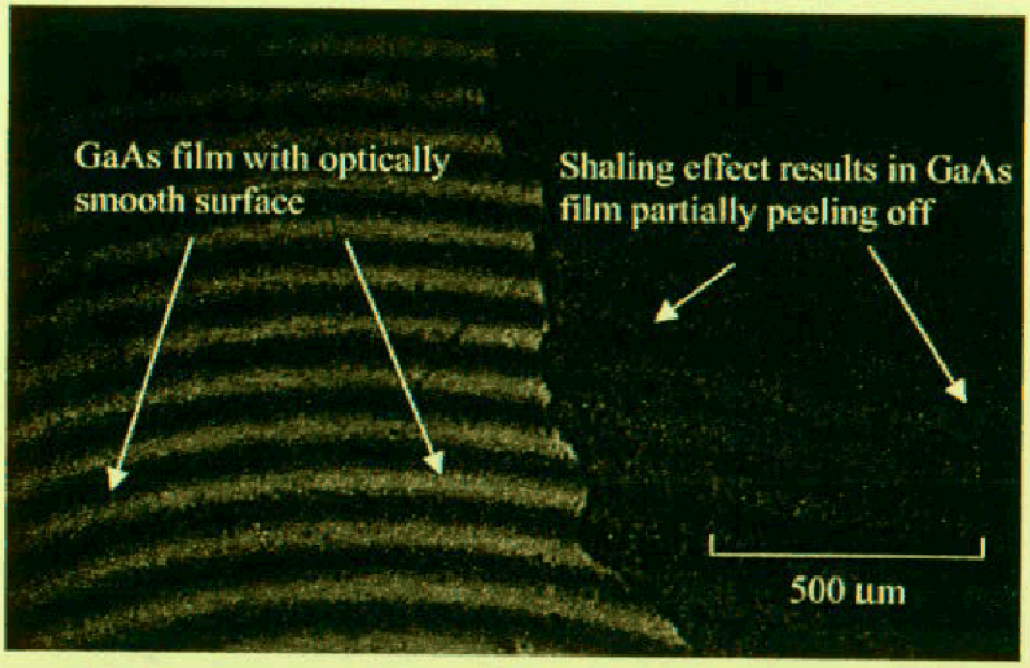
GaAs film with optically smooth surface
Shaling effect results in GaAs film partially peeling off
500 um

Figure 7

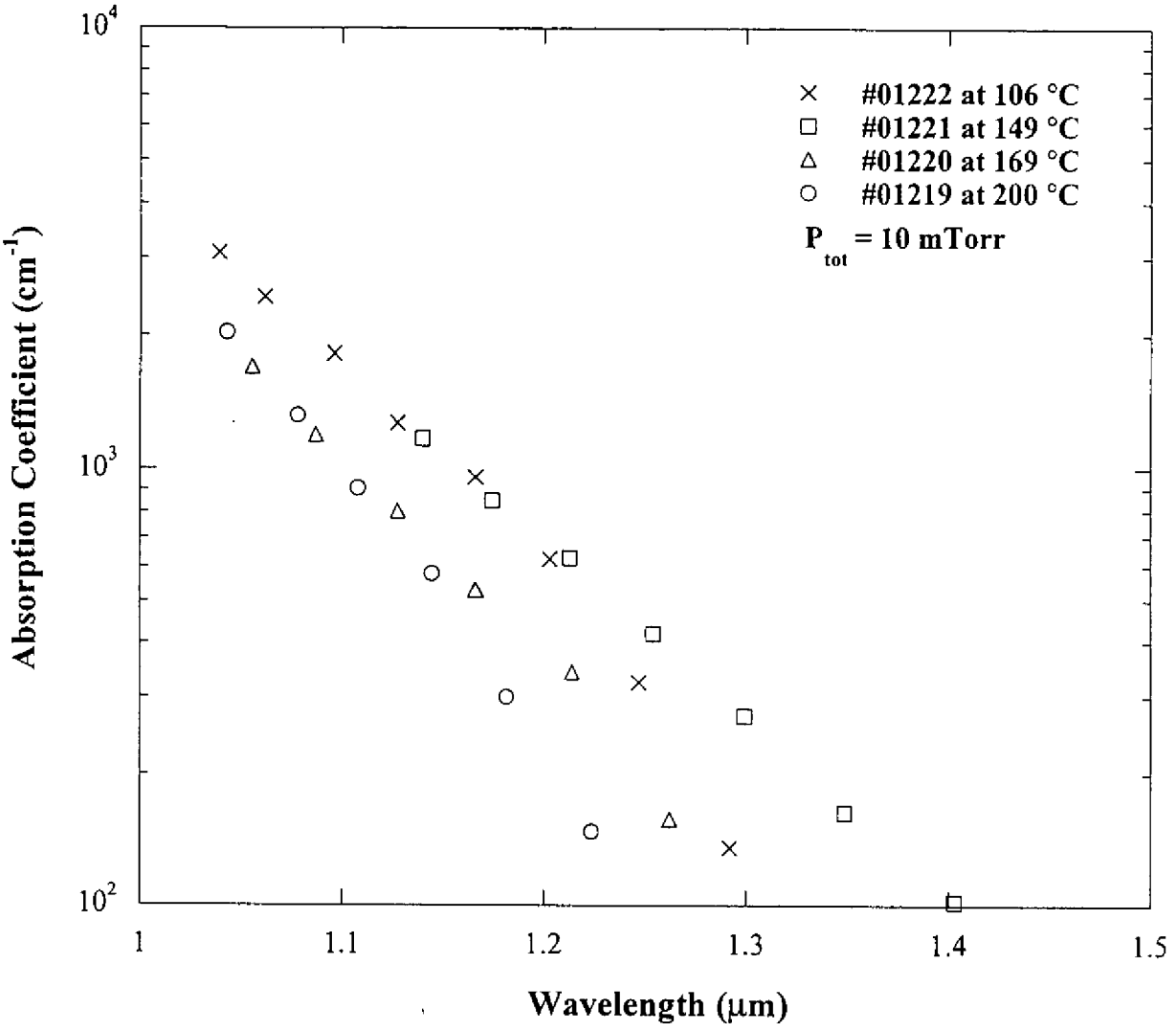
Absorption Coefficient (cm^{-1})
10^4
10^3
10^2
1
1.1
1.2
1.3
1.4
1.5
Wavelength (μm)
#01222 at 106 °C
#01221 at 149 °C
#01220 at 169 °C
#01219 at 200 °C
P_{tot} = 10 mTorr

Figure 8

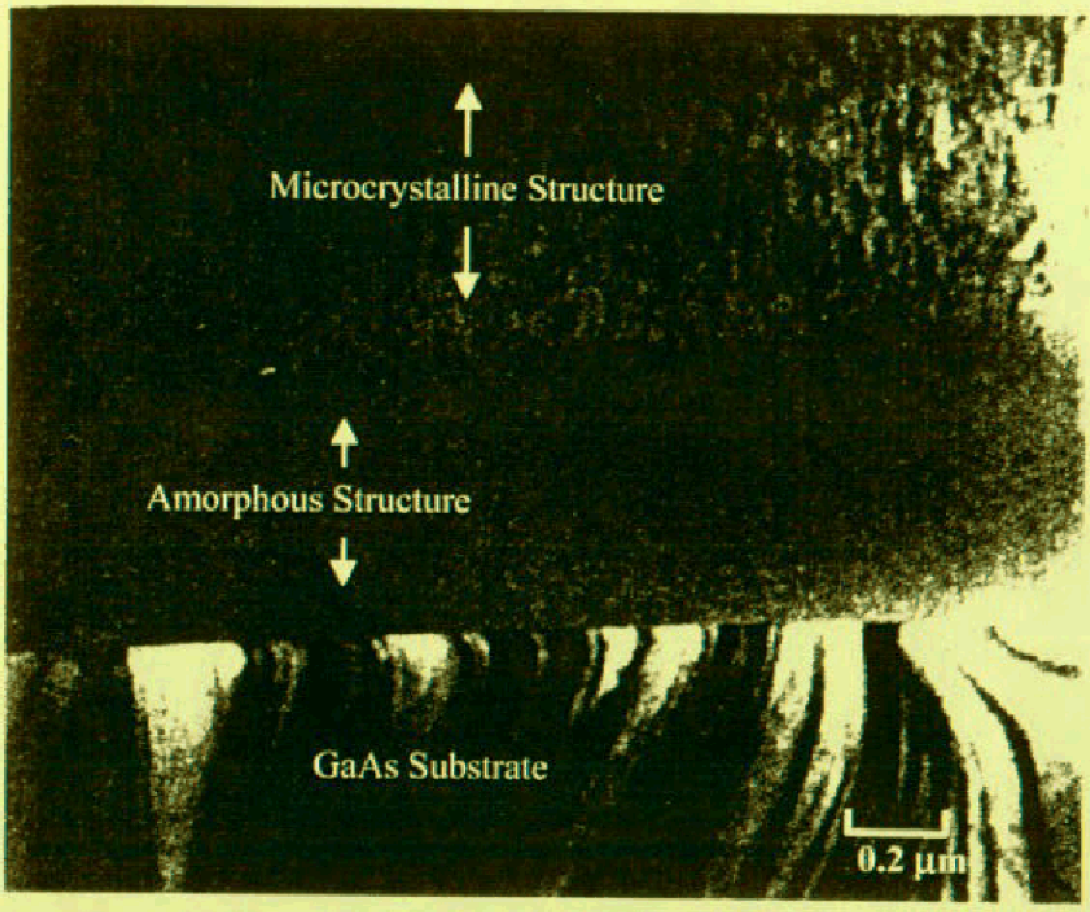
Microcrystalline Structure
Amorphous Structure
GaAs Substrate
0.2 µm

Figure 9

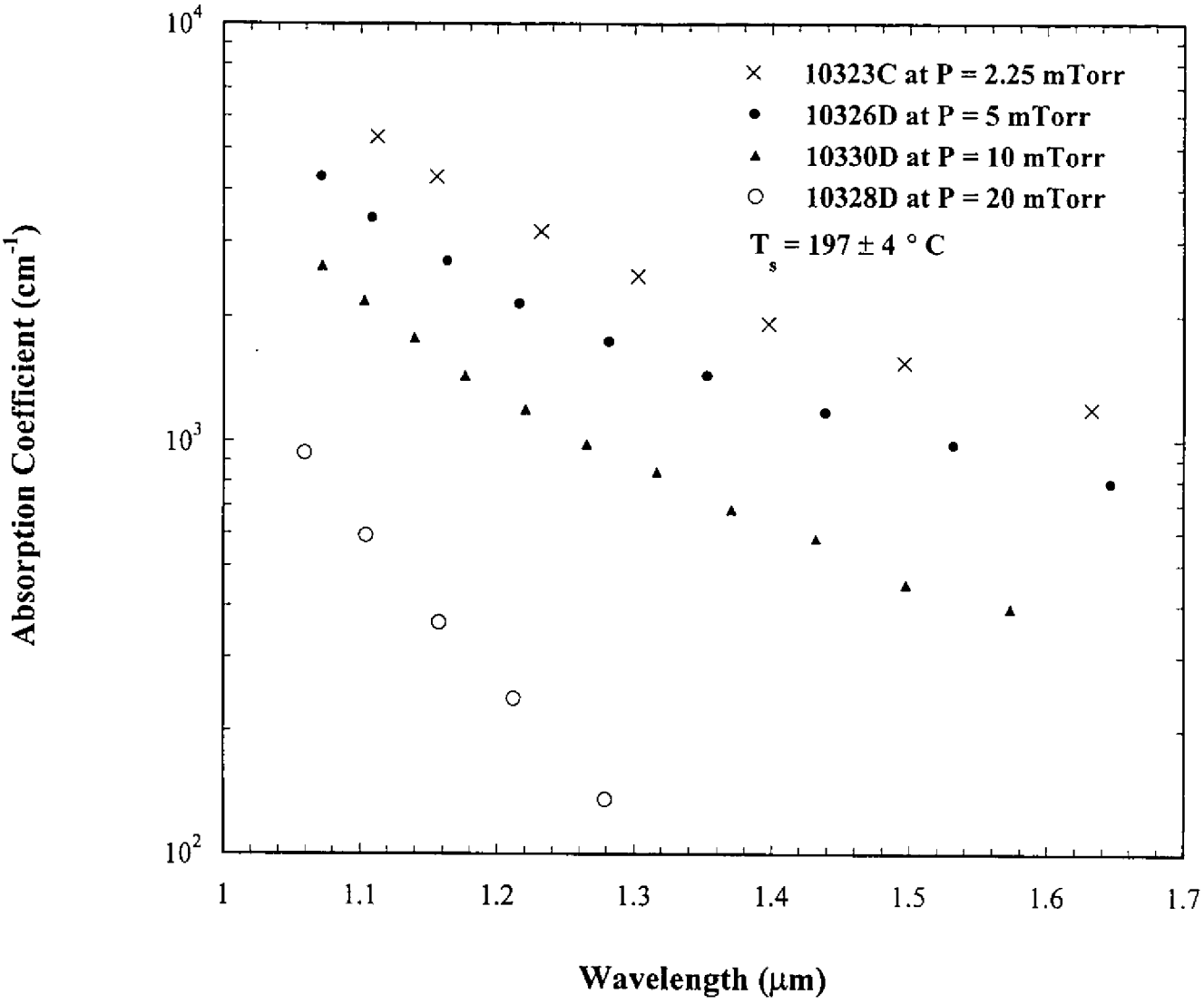
Absorption Coefficient (cm^{-1})
10^4
10^3
10^2
1
1.1
1.2
1.3
1.4
1.5
1.6
1.7
Wavelength (μm)
10323C at P = 2.25 mTorr
10326D at P = 5 mTorr
10330D at P = 10 mTorr
10328D at P = 20 mTorr
T_s = 197 ± 4 ° C

Figure 10

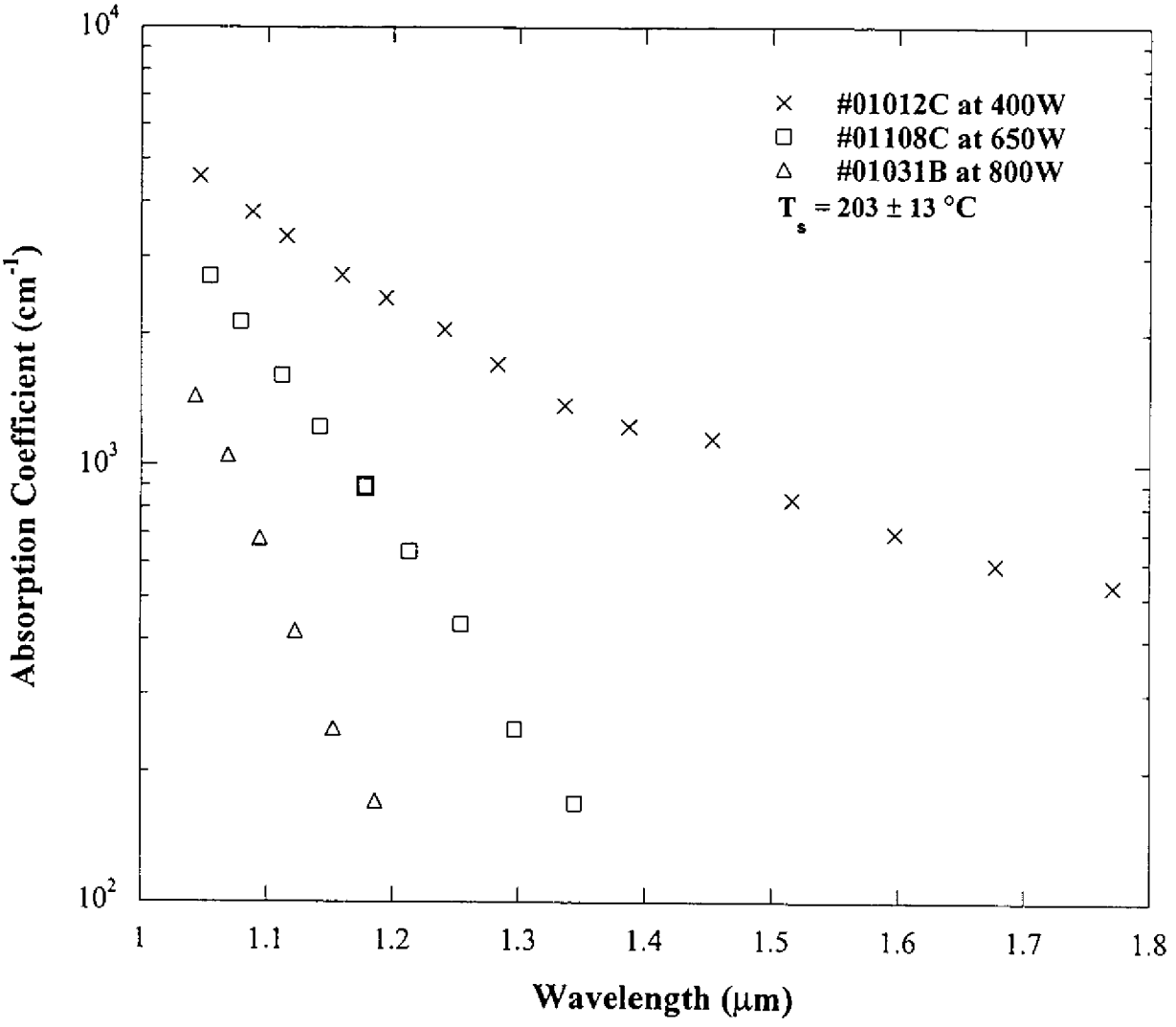
Absorption Coefficient (cm^{-1})
10^4
10^3
10^2
1
1.1
1.2
1.3
1.4
1.5
1.6
1.7
1.8
Wavelength (μm)
× #01012C at 400W
□ #01108C at 650W
△ #01031B at 800W
T_s = 203 ± 13 °C

Figure 11

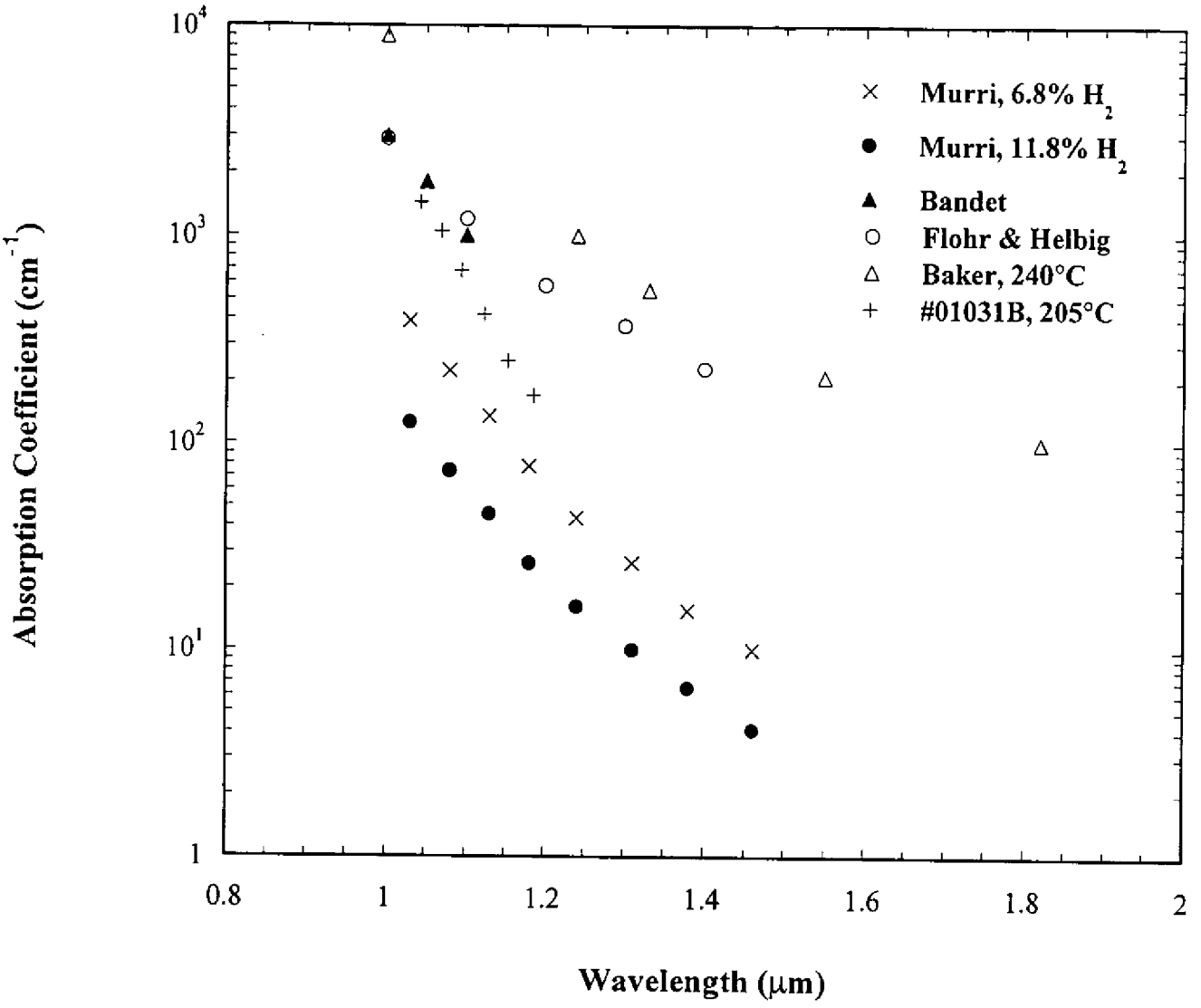
Absorption Coefficient (cm^{-1})
10^4
10^3
10^2
10^1
1
0.8
1
1.2
1.4
1.6
1.8
2
Wavelength (μm)
Murri, 6.8% H_2
Murri, 11.8% H_2
Bandet
Flohr & Helbig
Baker, 240°C
#01031B, 205°C

Figure 12